

NEW FINITE DEFORMATION MODEL FOR REINFORCED GRANULAR FILL OVER SUPER-SOFT RECLAIMED GROUND: I UNIFORMLY LOADED STRIP

K. Ramu¹, M. R. Madhav² and H. B. Poorooshab³

ABSTRACT: The presently available models for the analysis of reinforced foundation beds on soft ground are based on the infinitesimal deformation theory. A new model, which is extension and modification of Madhav & Poorooshab (1988) model is proposed to estimate the settlement response of a uniformly loaded strip on reinforced granular fill laid over a super-soft reclaimed ground and to estimate the mobilized tension in the reinforcement considering the hyperbolic stress–displacement response of the super soft soil, hyperbolic shear stress–shear strain response of the granular fill and finite deformation theory. The proposed model also considers shear stresses mobilized on the top and the bottom surfaces of the geosynthetic layer and relates them to the respective normal stresses. Results indicate that the infinitesimal theory underpredicts the displacements compared to those from the finite deformation theory. Parametric studies carried out quantify the effects of each parameter on the settlements along the reinforced foundation bed and tension mobilized in the reinforcement and facilitates design of footings on reclaimed ground.

Keywords: Reclaimed granular fill, super soft clay, reinforcement, mobilized tension, settlement, finite deformation theory

INTRODUCTION

Since the development of the reinforced earth concept (Vidal, 1966), numerous research projects have been undertaken to study the performance and behavior of reinforced soil structures. Yang (1972) proposed the equivalent confining and the anisotropic strength concepts. Binquet & Lee (1975) were the first to study the problem of bearing capacity of reinforced foundation bed systematically along with experimental validation. Nieuwenhuis (1977) proposed an analytical model for an embedded smooth membrane anchored at the ends for the problem assuming Boussinesq's stress distribution theory to be valid for the load applied on the surface. Basset & Last (1978) made a study of the soil below a footing, defined the strain field in terms of slip lines and suggested locations for the ideal placement of reinforcement. Giroud & Noiray (1981) have presented a simple approach for the design of unpaved roads for a large rut depth quantifying the membrane effect of the reinforcement in combination with load spread angle, heaving of the adjacent soil, etc. Milligan et al. (1989) have given an insight in to the Giroud & Noiray (1981) approach for small rut depths. They have established that

the applied vertical stresses cause shear stresses at the interface of the base and the sub-base material, which weaken the response of the soft soil. Reinforcement placed at the interface prevents lateral spreading of the soil above and improves the load carrying capacity of the soft ground.

Madhav & Poorooshab (1988) proposed a new model for the analysis of a footing on a reinforced granular bed. The subgrade soil, the granular bed and the reinforcement have been modelled by Winkler springs, Pasternak shear layer and rough membrane respectively. The results indicate that at small displacements, the contribution of shear layer far outweighs the effect of membrane action of the reinforcement in reducing the settlements of the reinforced soft soil. These results are in consonance with the observations of Jarrett (1980) and Boutrup and Holtz (1983). The effect of the reinforcement is significant at higher loads and large settlements. Ghosh & Madhav (1994a&b) extended the Madhav and Poorooshab (1988) model by incorporating a non-linear stress – displacement relation for soft soil and a non- linear shear stress – shear strain response for the granular fill and quantified the combined effects of the system on the response of the footing resting on the

¹ JNT University College of Engineering, Kakinada, Department of Civil Engineering, JNT University College of Engineering Kakinada, 533 003, Andhra Pradesh, INDIA

² IALT member, JNT University College of Engineering, Kukatpally, Department of Civil Engineering, JNT University College of Engineering, Kukatpally, 500 085, Andhra Pradesh, INDIA

³ IALT member, Concordia University, Montreal, CANADA

Note: Discussion on this paper is open until June 2009

reinforced granular bed. Shukla & Chandra (1994a&b) presented extension to the above model considering simultaneously the compressibility of the granular fill and prestress in the geosynthetic reinforcement. Yin (1997a) presented a further extension of Madhav & Poorooshasb (1988) model and satisfied the compatibility of displacements at the interface of the fill and the reinforcing layer. Yin (1997b) further modified the model (Yin, 1997a) by considering the non-linear responses of the soil and the fill.

Yin (2000) modeled the reinforced granular bed as a Timoshenko beam on elastic foundation. An analytic solution is obtained for a point load on an infinite Timoshenko beam on elastic foundation. Results from the Timoshenko beam (TB) model are compared with those from the finite element method and pure bending model (Winkler model based on pure or simple bending theory, PB). The results from the TB model are in good agreement with those from the FE model.

All the models presently available are developed based on infinitesimal deformation theory. As the reclaimed ground is very soft it undergoes large deformations especially at moderate to large loads. In such cases, the infinitesimal deformation theory may not be appropriate nor give good results. Therefore, in this study, a new extended model is proposed incorporating a finite deformation approach to estimate the complete

load-settlement response and the ultimate bearing capacity of a footing resting on a reinforced granular bed overlying super-soft reclaimed ground. The hyperbolic stress-displacement response of the soft ground and the hyperbolic shear stress-shear strain response of the granular bed are considered representing their responses by elasto-plastic Winkler model and Pasternak shear layer respectively. Full mobilization of interface shear resistance at interface of the fill and the reinforcement is assumed. Since the ground is very soft, very large settlements are expected during the placement of the granular fill and hence the problem is formulated as a moving boundary problem. For each incremental value of intensity of load, the settlement profile changes. The basic governing differential equations are developed by updating the profile for each increment of load intensity.

PROPOSED MODEL AND ANALYSIS

A strip load of width, $2B$, carrying an intensity of load, q , resting on the reinforced granular fill of thickness, H , and width, $2L$, overlaying super-soft reclaimed ground (Fig. 1a) is considered. The reinforcement (geosynthetic) layer is placed in the fill at a depth, H_r , from the top of the fill, and is of length $2L_r$ ($L_r = L$). The above system is modeled (Fig. 1.b)

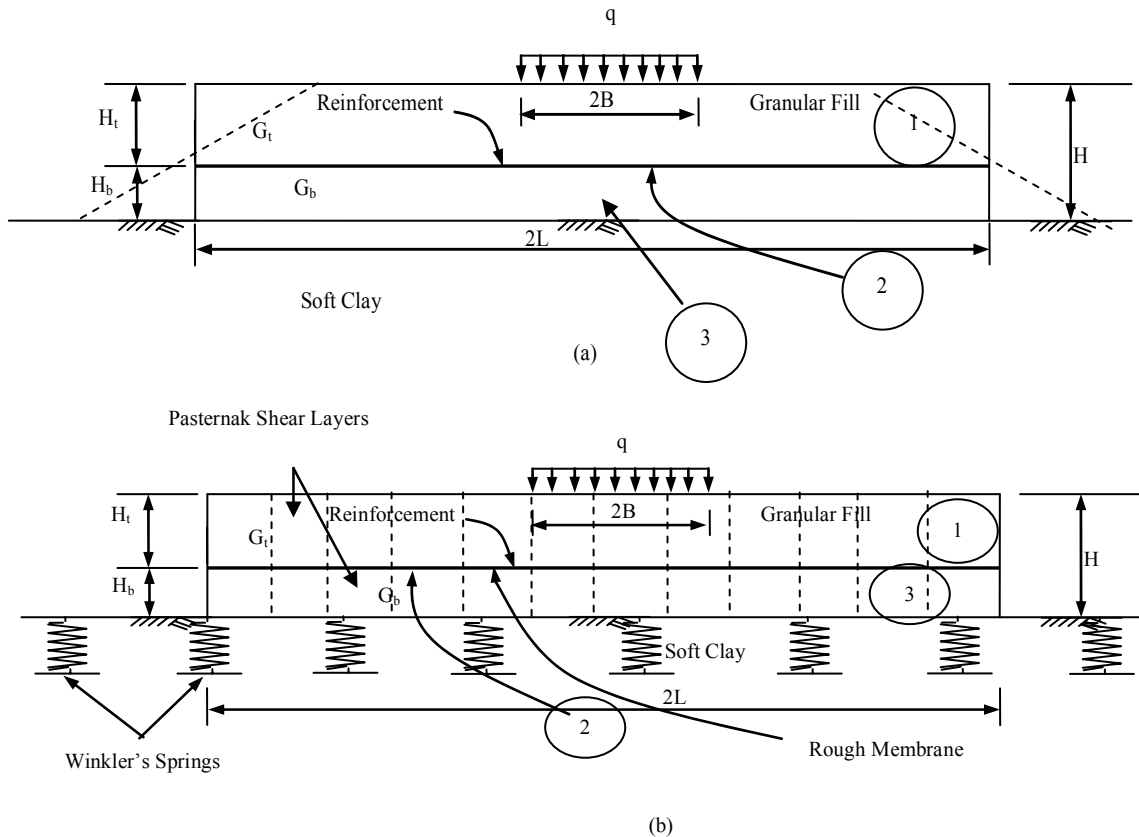


Fig. 1 (a) Footing on a reinforced granular fill – super-soft reclaimed soil system and (b) the proposed model

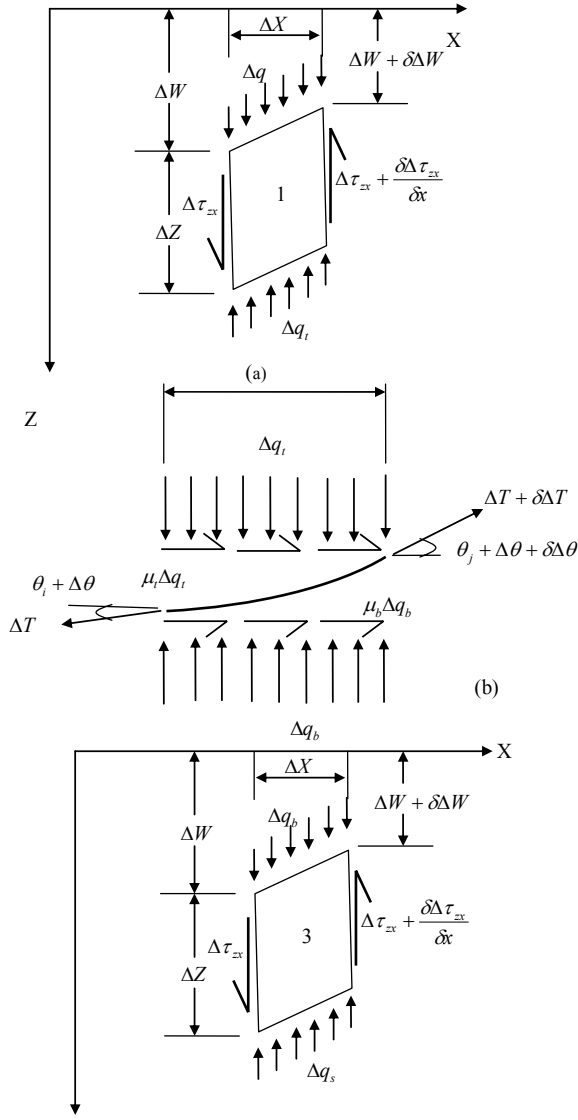


Fig. 2 Stresses in (a) the granular fill above reinforcement, element 1; (b) the reinforcement, element (2); (c) the granular fill below the reinforcement, element (3)

according to Madhav and Poorooshasb (1988) to consist of a shear layer, Winkler springs and a rough membrane to represent the granular fill, super-soft ground and a geosynthetic layer respectively.

The reinforced granular fill system is divided into three elements (1), (2) and (3), for the purpose of analysis. The three elements are the fill above the reinforcement, the reinforcement and the fill below the reinforcement respectively. The forces in the elements (1), (2) and (3), are depicted in Figs. (2a), (2b) and (2c) respectively.

With an incremental load of intensity, Δq , the governing equation for the equilibrium of element (1), using Pasternak shear layer concept can be written as

$$\Delta q = \Delta q_t + \frac{\partial \Delta N_x}{\partial x} \quad (1)$$

where Δq_t is the normal stress at the bottom of the element (1), i.e. above the reinforcement, $\partial \Delta N_x / \partial x$ is the variation of shear force along the vertical face of the element 1. The incremental shear force acting on the shear layer of thickness, H_t , is

$$\Delta N_x = \int_0^{H_t} \Delta \tau_{zx} dz \quad (2)$$

Assuming incremental shear stress, $\Delta \tau_{zx}$, to be constant along the depth, H_t , of the granular fill, Eq. (2) becomes

$$\Delta N_x = \Delta \tau_{zx} H_t \quad (3)$$

The shear stress - shear strain response of the granular fill idealized as a hyperbolic relation (Kondner, 1963) as shown in Fig. 3 and is expressed as

$$\tau_{zx} = \frac{\gamma_{zx}}{(c + d\gamma_{zx})} \quad (4)$$

where τ_{zx} and γ_{zx} are the shear stress and shear strain in the granular fill respectively and 'c' and 'd' are coefficients.

The reciprocal of the initial tangent modulus, G_t (shear modulus of the fill above reinforcement), is equal to 'c' while the reciprocal of the asymptotic value of shear stress, τ_f (ultimate shear resistance of the fill above the reinforcement) is equal to 'd'. Substituting for 'c' and 'd' in Eq. (4), one gets

$$\tau_{zx} = \frac{\gamma_{zx}}{\left(1/G_t + \frac{1}{\tau_f} \gamma_{zx}\right)} \quad (5a)$$

or

$$\tau_{zx} = \frac{G_t \gamma_{zx}}{\left(1 + \frac{G_t}{\tau_f} \gamma_{zx}\right)} \quad (5b)$$

Defining a non-linear parameter for the granular fill, $\beta_g = (G_t/\tau_f)$, Eq. (5b), becomes

$$\tau_{zx} = \frac{G_t \gamma_{zx}}{(1 + \beta_g \gamma_{zx})} \quad (6)$$

Differentiating Eq. (6) with respect to γ_{zx} , the incremental shear stress, $\Delta \tau_{zx}$, in the granular fill is

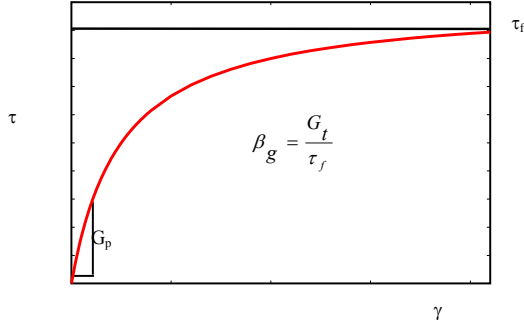


Fig. 3 Relation between shear stress and shear strain

$$\Delta\tau_{zx} = \frac{G_t \Delta\gamma_{zx}}{(1 + \beta_g \gamma_{zx})^2} \quad (7)$$

where, $\Delta\gamma_{zx}$ is the incremental shear strain respectively of the granular fill. Substituting Eq. (7) in Eq. (3), one can get

$$\Delta N_x = \frac{G_t H_t}{(1 + \beta_g \gamma_{zx})^2} \Delta\gamma_{zx} \quad (8)$$

The change in the displacement profile of an infinitesimal element of width, Δx , is shown in Fig. 4a, when the uniform stress on the footing increases from 'q' to 'q+ Δq '. The position of the infinitesimal element of length, Δx , (Fig. 4b), under the applied stress, q, is CD. The element displaces to EF when the stress becomes (q+ Δq). Line EI is horizontal while EG is parallel to CD. Since the shear layer is assumed to undergo only vertical displacements with negligible horizontal displacements, the shear strain is

$$\tan \gamma_{xz} \approx \gamma_{xz} = \frac{dw}{dx} \quad (9)$$

where w is the settlement at a distance, x, from the center of the loading. Only for infinitesimal values of shear strain is, $\tan \gamma_{xz} = \gamma_{xz}$. As the applied stress increases to (q+ Δq), the displacements of A and B increase respectively to w (q+ Δq , x) and w (q+ Δq , x+ Δx). The shear strain now is $\gamma_{xz} + \Delta\gamma_{xz}$. From the triangle EFI,

$$\tan(\gamma_{xz} + \Delta\gamma_{xz}) = \frac{dw + d\Delta w}{dx} \quad (10a)$$

or

$$\frac{\tan \gamma_{xz} + \tan \Delta\gamma_{xz}}{1 - \tan \gamma_{xz} \tan \Delta\gamma_{xz}} = \frac{dw}{dx} + \frac{d\Delta w}{dx} \quad (10b)$$

where $d\Delta w$ is the increment in displacement of point B with respect to point A under the stress increment of Δq . Simplifying Eq. (10b), one can get

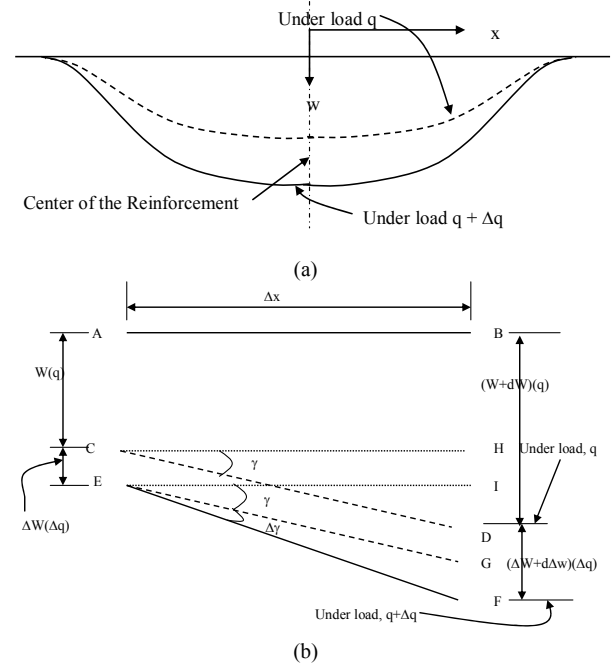


Fig. 4(a) Displacement profile of reinforcement under incremental loads; (b) idealization of displacement profiles

$$\tan \Delta\gamma_{xz} \cong \Delta\gamma_{xz} = \frac{\frac{d\Delta w}{dx}}{\left(1 + \tan^2 \gamma_{zx} + \tan \gamma_{zx} \frac{d\Delta w}{dx}\right)} \quad (11)$$

Substituting for $\Delta\gamma_{zx}$ from Eq. (11) in Eq. (8), one can get

$$\Delta N_x = \frac{G_t H_t}{(1 + \beta_g \gamma_{zx})^2} \frac{\frac{d\Delta w}{dx}}{\left(1 + \tan^2 \gamma_{zx} + \tan \gamma_{zx} \frac{d\Delta w}{dx}\right)} \quad (12)$$

The variation in increment in shear force on the vertical face of the element (1) can be obtained by differentiating Eq. (12) with respect to x as

$$\frac{\partial \Delta N_x}{\partial x} = -G_t H_t \left[\frac{c_1 \frac{d^2 \Delta w}{dx^2} + c_2 \frac{d\Delta w}{dx} \frac{d^2 w}{dx^2}}{(1 + \beta_g \gamma_{zx})^2 c_3^2} \right] \quad (13)$$

where $c_1 = 1 + \tan^2 \gamma_{xz}$

$$c_2 = \left\{ \left(2 \tan \gamma_{xz} + \frac{d\Delta w}{dx} \right) + \frac{2\beta_g}{(1 + \beta_g \gamma_{xz})} c_3 \cos^2 \gamma_{xz} \right\} \text{ and}$$

$$c_3 = \left(1 + \tan^2 \gamma_{xz} - \tan \gamma_{xz} \frac{d\Delta w}{dx} \right)$$

Substituting Eq. (13) in Eq. (1) one gets,

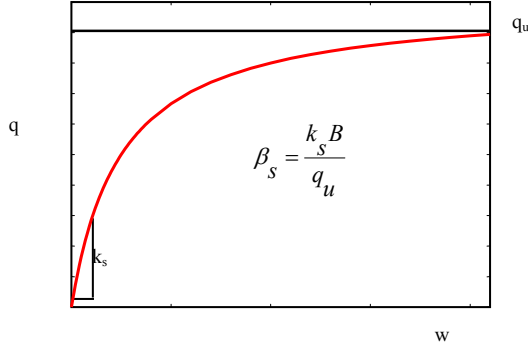


Fig. 5 Relation between intensity of load and settlement

$$\Delta q = \Delta q_t - G_t H_t \left[\frac{c_1 \frac{d^2 \Delta w}{dx^2} + c_2 \frac{d \Delta w}{dx} \frac{d^2 w}{dx^2}}{(1 + \beta_g \gamma_{xz})^2 c_3^2} \right] \quad (14)$$

Similarly by considering the vertical force equilibrium of element 3 (Fig. 2c, fill below the reinforcement layer), the governing equation is obtained as

$$\Delta q_s = \Delta q_b + G_b H_b \left[\frac{c_1 \frac{d^2 \Delta w}{dx^2} + c_2 \frac{d \Delta w}{dx} \frac{d^2 w}{dx^2}}{(1 + \beta_{gb} \gamma_{zx})^2 c_3^2} \right] \quad (15)$$

where Δq_b and Δq_s are the vertical normal stresses at the top and bottom of the fill below the reinforcement, G_b , H_b , τ_{fb} and β_{gb} are the initial shear modulus, thickness of the granular fill, the ultimate shear resistance and non-linear parameter, ($= G_b/\tau_{fb}$) respectively of the fill below the reinforcement.

The stress-displacement response of the super-soft deposit is represented by a hyperbolic relation as shown in Fig. 5 (Kondner, 1963) as

$$q = \frac{w}{(a + bw)} \quad (16)$$

where 'w' is the settlement, 'q' is the applied vertical stress, 'a' and 'b' are the coefficients. Both these coefficients 'a' and 'b' have physical meanings. The reciprocal of the initial tangent modulus, k_s (subgrade modulus) is equal to 'a' while the reciprocal of the ultimate (asymptotic) value of stress, q_u , (ultimate bearing capacity) is b. $q_u = c_u N_c$, - the ultimate bearing capacity of the footing on super-soft ground, c_u - undrained strength of soft soil and N_c - the bearing capacity factor.

Substituting the values of coefficients 'a' and 'b' in

Eq. 16, one gets

$$q_s = w / (1/k_s + w/q_u) = \frac{k_s w}{\left(1 + \frac{k_s}{q_u} w\right)} \quad (17)$$

With $\beta_s = k_s B/q_u$, where β_s is a non-linear parameter of the super-soft reclaimed soil, Eq. (17) becomes

$$q_s = \frac{k_s w}{\left(1 + \beta_s \frac{w}{B}\right)} \quad (18)$$

Differentiating Eq. (18) with respect to w, the increment in resistance, Δq_s , of the super-soft soil is

$$\Delta q_s = \frac{k_s \Delta w}{(1 + \beta_s w)^2} \quad (19)$$

where Δw is the incremental settlement.

Considering the reinforcement in the reinforced granular fill, i.e. element (2), (Fig. 2b), the horizontal force equilibrium requires,

$$\frac{d \Delta T}{dx} \text{Cos}(\theta + \Delta \theta) - \Delta T \text{Sin}(\theta + \Delta \theta) \frac{d \Delta \theta}{dx} = -(\mu_t \Delta q_t + \mu_b \Delta q_b) - (\Delta c_{at} + \Delta c_{ab}) \quad (20)$$

where θ and $\Delta \theta$ are the inclinations of the deformed shape of the granular fill at the end of the previous lift and the incremental inclination of the deformed element caused by the incremental load, Δq , respectively. μ_t and Δc_{at} are the frictional and adhesive resistances respectively at the interface between the top granular fill and the reinforcement, μ_b and Δc_{ab} are the frictional and adhesive resistances respectively at the interface of the bottom granular fill and the reinforcement, ΔT is the increase in tension in the reinforcement with the increase in intensity of load, Δq . Similarly, from the vertical equilibrium of the forces in the reinforcement element (2), one gets

$$\frac{d \Delta T}{dx} \text{Sin}(\theta + \Delta \theta) + \Delta T \text{Cos}(\theta + \Delta \theta) \frac{d \Delta \theta}{dx} = (\Delta q_t - \Delta q_b) \quad (21)$$

Multiplying Eq.s (20) by $\text{Cos}(\theta + \Delta \theta)$ and Eq. (21) by $\text{Sin}(\theta + \Delta \theta)$ and adding, one obtains

$$\frac{d \Delta T}{dx} = (\Delta q_t - \Delta q_b) \text{Sin}(\theta + \Delta \theta) - (\mu_t \Delta q_t + \mu_b \Delta q_b + \Delta c_{at} + \Delta c_{ab}) \text{Cos}(\theta + \Delta \theta) \quad (22)$$

Similarly multiplying Eq.s (20) by $\text{Sin}(\theta + \Delta\theta)$ and (21) by $\text{Cos}(\theta + \Delta\theta)$ and subtracting Eq. (22) from Eq. (23) the following equation can be obtained,

$$\begin{aligned} \Delta T \frac{d\Delta\theta}{dx} &= \text{Sin}(\theta + \Delta\theta) \{ \mu_t \Delta q_t + \mu_b \Delta q_b + \Delta c_{at} + \Delta c_{ab} \} \\ &+ \text{Cos}(\theta + \Delta\theta) \{ \Delta q_t - \Delta q_b \} \end{aligned} \quad (23)$$

Rearranging the terms of Eq. (22), one gets

$$\begin{aligned} \frac{d\Delta T}{dx} &= -\{ \mu_t \text{Cos}(\theta + \Delta\theta) - \text{sin}(\theta + \Delta\theta) \} \Delta q_t \\ &- \{ \mu_b \text{Cos}(\theta + \Delta\theta) + \text{sin}(\theta + \Delta\theta) \} \Delta q_b \\ &- \text{Cos}(\theta + \Delta\theta) \{ \Delta c_{at} + \Delta c_{ab} \} \end{aligned} \quad (24)$$

Rearranging the terms of Eq. (23), one gets

$$\begin{aligned} \Delta T \frac{d\Delta\theta}{dx} &= -\{ \mu_t \text{Sin}(\theta + \Delta\theta) + \text{Cos}(\theta + \Delta\theta) \} \Delta q_t \\ &- \{ \mu_b \text{Sin}(\theta + \Delta\theta) - \text{Cos}(\theta + \Delta\theta) \} \Delta q_b \end{aligned} \quad (25a)$$

or

$$\begin{aligned} \Delta q_t &= \left\{ \frac{1 - \mu_b \text{Tan}(\theta + \Delta\theta)}{1 + \mu_t \text{Tan}(\theta + \Delta\theta)} \right\} \Delta q_b \\ &- \Delta T \frac{d\Delta\theta}{dx} \frac{1}{\text{Cos}(\theta + \Delta\theta) + \mu_t \text{Sin}(\theta + \Delta\theta)} \end{aligned} \quad (25b)$$

Substituting Eq.s (14) and (15) in Eq. (24), one gets

$$\begin{aligned} \frac{d\Delta T}{dx} &= -(\mu_t \text{cos}(\theta + \Delta\theta) - \text{sin}(\theta + \Delta\theta)) * \\ &\left[\Delta q + G_t H_t \left(c_2 \frac{d^2 \Delta w}{dx^2} - \frac{d\Delta w}{dx} (c_3 + c_4) \frac{d^2 \Delta w}{dx^2} \right) / c_1^2 \right] \\ &- (\mu_b \text{cos}(\theta + \Delta\theta) - \text{sin}(\theta + \Delta\theta)) * \\ &\left[\frac{k_s \Delta w}{(1 + \beta_s w/B)^2} + G_b H_b \left(c_2 \frac{d^2 \Delta w}{dx^2} - \frac{d\Delta w}{dx} (c_3 + c_4) \frac{d^2 \Delta w}{dx^2} \right) / c_1^2 \right] \\ &- \text{Cos}(\theta + \Delta\theta) \{ \Delta c_{at} + \Delta c_{ab} \} \end{aligned} \quad (26)$$

Equation (26) relates the variation of the incremental tensile force in the reinforcement to the incremental load of intensity, Δq . The corresponding equation by infinitesimal deformation theory (Ramu, 2001) is

$$\begin{aligned} \frac{dT}{dx} &= -(\mu_t \text{cos} \theta - \text{sin} \theta) \left[q + \frac{G_t H_t}{\left(1 + \beta_g \frac{dw}{dx}\right)^2} \frac{d^2 w}{dx^2} \right] \\ &- (\mu_b \text{cos} \theta + \text{sin} \theta) \left[\frac{k_s w}{1 + \beta_s \frac{w}{B}} \right] - (C_{at} + C_{ab}) \text{cos} \theta \end{aligned} \quad (27)$$

Equation (27) is the governing equation for variation of tensile force in the reinforcement along the length from the center of the reinforcement. C_{at} and C_{ab} are the adhesive resistances on the top and the bottom interfaces of the reinforcement.

Substituting Eq. (14) and (15) in Eq. (25b), and simplifying, the expression becomes

$$\begin{aligned} \Delta q &= - \left[\left(G_t H_t + G_b H_b \left\{ \frac{1 + \mu_b \text{tan}(\theta + \Delta\theta)}{1 - \mu_t \text{tan}(\theta + \Delta\theta)} \right\} \right) * \right. \\ &\left. \left[\left(c_2 \frac{d^2 \Delta w}{dx^2} - \frac{d\Delta w}{dx} (c_3 + c_4) \frac{d^2 \Delta w}{dx^2} \right) / c_1^2 \right] \right. \\ &- \left. \left\{ \frac{\Delta T \text{cos}^2 \Delta \gamma_{xx}}{\text{cos}(\theta + \Delta\theta) - \mu_t \text{sin}(\theta + \Delta\theta)} \right\} \left(c_2 \frac{d^2 \Delta w}{dx^2} - \frac{d\Delta w}{dx} c_3 \frac{d^2 \Delta w}{dx^2} \right) / c_3^2 \right. \\ &\left. + \frac{k_s \Delta w}{(1 + \beta_s w/B)^2} \left\{ \frac{1 + \mu_b \text{tan}(\theta + \Delta\theta)}{1 - \mu_t \text{tan}(\theta + \Delta\theta)} \right\} \right] \end{aligned} \quad (28)$$

The corresponding equation by the infinitesimal theory is

$$\begin{aligned} q &= \left(\frac{1 - \mu_b \text{cos} \theta}{1 + \mu_t \text{cos} \theta} \right) \frac{k_s w}{1 + \beta_s w/B} - \frac{\text{tan} \theta}{1 + \mu_t \text{cos} \theta} (C_{at} + C_{ab}) \\ &- \left[\frac{G_t H_t}{\left(1 + \beta_g \frac{dw}{dx}\right)^2} + \frac{G_b H_b}{\left(1 + \beta_g \frac{dw}{dx}\right)^2} \left(\frac{1 - \mu_b \text{cos} \theta}{1 + \mu_t \text{cos} \theta} \right) + \frac{T \text{cos} \theta}{1 + \mu_t \text{cos} \theta} \right] \frac{d^2 w}{dx^2} \end{aligned} \quad (29)$$

Equation (29) is the governing equation for intensity of load on the reinforced granular bed.

Normalizing with $q^* = q/k_s B$, $W = w/B$, $X = x/B$, $\Delta X = \Delta x/B$, $\Delta W = \Delta w/B$, $\Delta q^* = \Delta q/k_s B$, $\Delta T^* = \Delta T/k_s B^2$ and $G_t^* = G_t H_t/k_s B^2$, $G_b^* = G_b H_b/k_s B^2$, Eq.s. (28) and (26) become

$$\Delta q^* = - \left[\left(G_t^* + G_b^* \left\{ \frac{1 + \mu_b \tan(\theta + \Delta\theta)}{1 - \mu_t \tan(\theta + \Delta\theta)} \right\} \right) \right]^*$$

$$\left[\left(c_2 \frac{d^2 \Delta W}{dX^2} - \frac{d\Delta W}{dX} (c_3^* + c_4^*) \frac{d^2 W}{dX^2} \right) / (c_1^*)^2 \right]^*$$

$$\left\{ \frac{\Delta T \cos^2 \Delta \gamma_{zx}}{\cos(\theta + \Delta\theta) - \mu_t \sin(\theta + \Delta\theta)} \right\} \left(c_2 \frac{d^2 \Delta W}{dX^2} - \frac{d\Delta W}{dX} c_3^* \frac{d^2 W}{dX^2} \right) / (c_5^*)^2$$

$$+ \frac{\Delta W}{(1 + \beta_s W)^2} \left\{ \frac{1 + \mu_b \tan(\theta + \Delta\theta)}{1 - \mu_t \tan(\theta + \Delta\theta)} \right\} \quad (30)$$

and

$$\frac{d\Delta T^*}{dX} = -(\mu_t \cos(\theta + \Delta\theta) - \sin(\theta + \Delta\theta))^*$$

$$\left[\Delta q^* + G_t^* \left(c_2 \frac{d^2 \Delta W}{dX^2} - \frac{d\Delta W}{dX} (c_3^* + c_4^*) \frac{d^2 W}{dX^2} \right) / (c_1^*)^2 \right]^*$$

$$- (\mu_b \cos(\theta + \Delta\theta) - \sin(\theta + \Delta\theta))^*$$

$$\left[\frac{\Delta W}{(1 + \beta_s W)^2} + G_b^* \left(c_2 \frac{d^2 \Delta W}{dX^2} - \frac{d\Delta W}{dX} (c_3^* + c_4^*) \frac{d^2 W}{dX^2} \right) / (c_1^*)^2 \right]^* \quad (31)$$

where $c_5^* = (1 + \tan^2 \gamma_{zx} - \tan \gamma_{zx} d\Delta W/dX)$;
 $c_1^* = c_5^* (1 + \beta_g \gamma_{zx})$; $c_3^* = (2 \tan \gamma_{zx} - d\Delta W/dX)$;
 $c_4^* = 2 \beta_g c_5^* \cos^2 \theta / (1 + \beta_g \gamma_{zx})$.

Four boundary conditions are required to solve the above two partial differential equations, (Eq.s 30 & 31). They are: at $x = 0$ or $X = 0$, i.e. at the center of the reinforced granular bed, the incremental displacement and the tensions are maximum. Hence, the slope of the settlement profile at this point is zero. i.e.,

$$d\Delta w/dx = 0 \text{ or } d\Delta W/dX = 0 \quad (32a)$$

and the slope of the tension – distance curve also is zero. i.e.,

$$d\Delta T/dx = 0 \text{ or } d\Delta T^*/dX = 0. \quad (32b)$$

At $x = L$ or $X = L^*$, i.e. at the edge of the reinforced granular fill, the slope of the settlement profile is zero, i.e.,

$$d\Delta w/dx = 0 \text{ or } d\Delta W/dX = 0 \quad (32c)$$

and the tension is zero at the free edge (the free end of the reinforcement). Hence

$$\Delta T = 0 \text{ or } \Delta T^* = 0 \quad (32d)$$

NUMERICAL EXPERIMENTATION

Equations (30) and (31) are non-linear and coupled and hence need to be solved numerically to evaluate the settlement and tension in the reinforcement at any point. Equation (30) and (31) are solved iteratively for each increment in stress, Δq^* , with the boundary conditions (Eq.s 32) to obtain the incremental settlements, ΔW . These incremental settlements are summed up to get the total settlement as

$$W_i^*(q + \Delta q) = W_i^*(q) + \Delta W_i^* \text{ for } 0 < i < nt+1 \quad (33)$$

where $W_i(q^*)$ and $W_i(q^* + \Delta q^*)$ are the normalized total settlements at node 'i' under the loads of intensity, q^* and $q^* + \Delta q^*$ respectively. Similarly, the increments in tensions are summed up to get the total mobilized tension as

$$T_i^*(q + \Delta q) = T_i^*(q) + \Delta T_i^* \text{ for } 0 < i < nt+1 \quad (34)$$

where $T_i(q^*)$ and $T_i(q^* + \Delta q^*)$ are the normalized tensions in the reinforcement at node 'i' under the loads of intensity, q^* and $q^* + \Delta q^*$ respectively.

For uniformly loaded footing, the incremental intensity of load, Δq^* , is specified over the width of the footing. In the first iteration Eq. (30) is solved assuming the incremental tension, ΔT_i , to be zero, thus determining ΔW_i . The tensions, ΔT_i , are then evaluated by solving Eq. (31) with the above computed displacements. In the subsequent iterations the previously evaluated tensions and displacements are substituted and new values obtained till the old and new values converge. The convergence criteria are

$$\frac{|\Delta W_i^k - \Delta W_i^{k-1}|}{\Delta W_i^k} \leq 0.000005 \quad (35a)$$

and

$$\frac{|\Delta T_i^k - \Delta T_i^{k-1}|}{\Delta T_i^k} \leq 0.000005 \quad (35b)$$

where ΔW_i^{k-1} & ΔW_i^k and ΔT_i^{k-1} & ΔT_i^k are respectively the normalized displacements and normalized tensions at node 'i' after $(k-1)^{th}$ and k^{th} iterations.

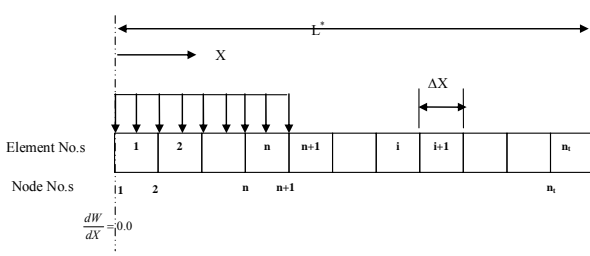


Fig. 6 Descretisation of the load and the reinforced granular bed

CONVERGENCE STUDY

The quantities W_i and T_i^* are estimated by varying the number of elements, n , into which half the width of the footing is divided. To minimize the numerical error, a convergence study is carried out, by varying the discretisation of the domain. The number of elements, n , is varied from 10 to 100. The results did not vary much except at large settlements and even at large settlement ($W \geq 1.0$) the solution converges for the number of elements, n , equal to or greater than 50. Hence the number of elements, ‘ n ’, into which the loaded region, B , is discretised is made equal to 50 in the subsequent analysis. A further study was then carried out with $n = 50$ but by varying the stress increment, Δq^* . The accuracy of the results improved with decreasing values of Δq^* . However, for $\Delta q^* < 0.0001$, no perceptible change in normalized settlement, W , was observed. Therefore all further analyses have been carried out with $n = 50$ and $\Delta q^* = 0.0001$.

RESULTS AND DISCUSSION

Only half the width of the reinforced zone is considered for the analysis considering symmetry of the applied load and of the reinforced zone. Half width of the loading, B , and the half width of the reinforced zones, L are divided into ‘ n ’ and ‘ nt ’ number of elements of equal length, Δx , as shown in Fig. 6. The loading boundary conditions are

$$\begin{aligned} \Delta q_i &= \Delta q && \text{for } 0 < i \leq n \\ \Delta q_i &= \Delta q/2.0 && \text{for } i = n+1 \\ \Delta q_i &= 0 && \text{for } n+1 < i \leq nt+1 \end{aligned}$$

Settlements of the reinforced foundation bed and tension developed in the reinforcement layer, under uniform loading are studied through a parametric study, for the following ranges of modulus of subgrade reaction, k_s , of soft ground shown in Table 1. The shear modulus

of the granular fill is varied from 1,500 to 50,000 kN/m². The interface friction angle between the reinforcement and the granular fill is from 0 to 45⁰ (smooth to perfectly rough membrane).

Normalized settlements of the reinforced foundation bed and the normalized tension developed in the reinforcement layer, under uniform loading are studied through a parametric study, for the following ranges of non-dimensional parameters $G_t^* = G_b^* = 0.05$ to 1.0; $\beta_s = 5$ to 100; $\beta_g = 5$ to 50; $q^* = 0.01$ to 0.2, $\mu_t = \mu_b = 0$ (smooth) to 1.0 (fully rough) membrane.

The modulus of subgrade reaction, k_s , the stiffness of the granular bed, G_t , and the ultimate bearing resistance, q_{ub} , and the interface bond resistance between the reinforcement and the fill, are the basic parameters which affect the physics of the problem and hence considered as they control the overall performance of the reinforced granular bed on super-soft ground to applied loads. The normal working ranges of the above parameters are estimated based on which the ranges of the normalized parameters worked out for the parametric study.

Three values of normalized shear stiffness of the granular fill on top, $G_t^* = 0.1, 0.2$ and 0.5 are considered to study the effect of the shear stiffness on the load intensity – settlement responses (Fig. 7) of the reinforced granular bed system, by both infinitesimal and finite deformation theories for $G_b^* = 0.1, \beta_s = 10, \beta_g = 5, \mu_t = \mu_b = 1.0$. The load intensity – settlement response curves at the middle of the reinforced granular bed ($X=0$), from both infinitesimal and finite deformation approaches are identical at small load intensities, i.e., in the absence of large or finite deformations. The response curves deviate from each other with increasing load intensity, the finite deformation theory predicting larger settlements than the infinitesimal approach. The load – settlement curves become steep with increasing stress and show definite ultimate bearing capacities of the system by the finite deformation theory while no such definite trend or values can be discerned from the responses based on the infinitesimal deformation theory. The differences in settlements from the two theories increase with decreasing shear stiffness, G_t^* , of the fill for any particular intensity of load. A decrease of shear stiffness of the fill causes a larger increase in the

Table 1 Typical values for the modulus of subgrade reaction, k_s , (kN/m³) for normally consolidated clay (after Terzaghi 1955)

Type of Soil	Modulus of Subgrade Reaction, k_s
Very Soft clays	1560 kN/m ³
Stiff clays	7800 kN/m ³

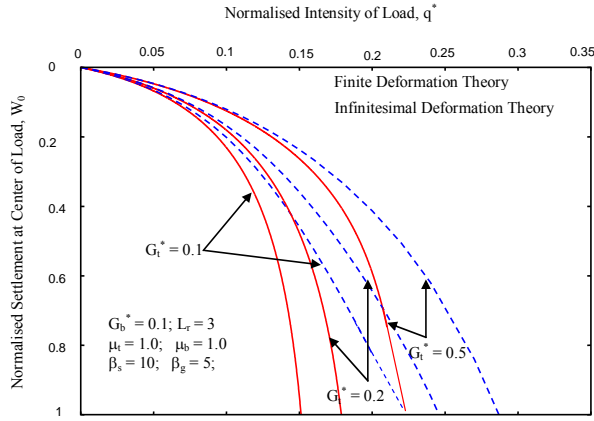


Fig. 7 Intensity of load, q^* , - settlement, W_0 , responses: effect of G_t^*

settlements from the finite deformation approach, resulting in increases in the differences in the values computed by the two theories.

The shear stiffness of the granular fill on top of the reinforcement has significant effect on the response curves (Fig. 7). Stiffer the granular fill, smaller would be the settlement under the load. At normalized intensity of load, $q^* = 0.15$, the normalized settlements, W_0 , at the center of the load, $X=0$, are 0.9415, 0.4762 and 0.2628 respectively for $G_t^* = 0.1, 0.2$ and 0.5 by the finite deformation theory. With increasing shear stiffness, G_t^* , of the fill, the settlement under the load decreases, since stiff granular fill distributes the load more uniformly, hence larger percentage of load is transferred to the area outside the loaded area, leading to a decrease in the settlement under the loaded region.

The variation of mobilized tension at the center, T_0^* , of the loading showing the effect of shear stiffness, G_t^* , of the fill above the reinforcement, with the intensity of load, q^* , is depicted in Fig. 8. The constant parameters are shear stiffness of the fill below the reinforcement, $G_b^* = 0.01$, $\beta_s = 10$, $\beta_g = 5$, $\mu_t = \mu_b = 1.0$. The variation of mobilized tension, T_0^* , with q^* , is linear and the differences between curves corresponding to

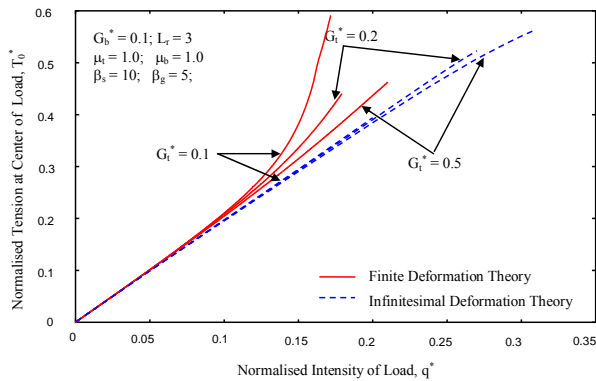


Fig. 8 Intensity of load, q^* , - tension, T_0^* , responses: effect of G_t^*

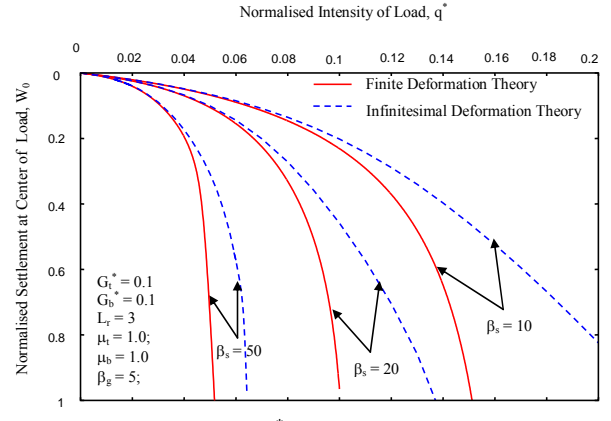


Fig. 9 Intensity of load, q^* , - settlement, W_0 , responses: effect of β_s

infinitesimal and finite deformation approaches are very small upto an intensity of load equal to $q^* = 0.1$ by the finite deformation theory and 0.15 by the infinitesimal deformation theory. At small intensities of loads, the differences in normalized mobilized tensions are very less, since the differences in settlements are very small and the load to be transferred by the reinforcement is also very less. At normalized intensity of load, $q^* = 0.15$, the normalized tensions, T_0^* , at the center of the loading are 0.3811, 0.3359 and 0.315 respectively for $G_t^* = 0.1, 0.2$ and 0.5 by the finite deformation theory. With the increase in shear stiffness of the fill, the mobilized tension decreases, since the stiff granular fill distributes the load more uniformly, the differential settlement reduces leading to less mobilization of shear stresses and tension. The tension curves by the finite deformation theory are concave upwards, indicating that the tension increases rapidly with increase in intensity of load may be because at a particular load, the granular fill reaches its ultimate load transfer capacity with the result the reinforcement actively starts transferring the loads causing more tension to be mobilized in the reinforcement. In the case of infinitesimal theory, the mobilized tensions continue to increase gradually even at an intensity of load of $q^* = 0.2$.

The effect of the ultimate bearing capacity, q_u , of the super-soft reclaimed soil on the load intensity – central settlement, W_0 , response of the reinforced granular bed is studied through the parameter $\beta_s (=k_s B/q_u)$ in Fig. 9, for $G_t^* = 0.1$, $G_b^* = 0.1$, $\beta_g = 5$ and $\mu_t = \mu_b = 1.0$. Three values of $\beta_s = 10, 20$ and 50 corresponding to strong to weak ground, are considered. An increase in β_s indicates a decrease in ultimate bearing capacity, q_u , of the super-soft soil resulting in an increase of settlement. The settlements obtained by the infinitesimal deformation theory are always less than those obtained by the finite deformation theory, the differences in the values of settlements from the finite and infinite deformation

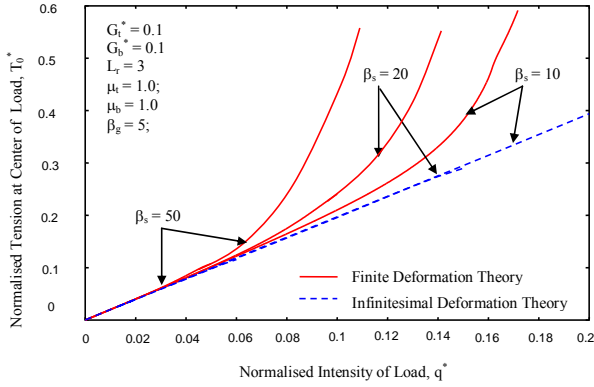


Fig. 10 Intensity of load, q^* - tension, T_0^* , responses: effect of β_s

theories increase with increasing settlement. The differences in the settlements from finite and infinitesimal deformation theories increase with increase in β_s since an increase of β_s corresponds to a decrease in the ultimate bearing capacity of the reclaimed soil. The loads carried by the reinforced granular bed system at a normalized settlement of 0.4 are 0.1232, 0.0847 and 0.0468 respectively for $\beta_s = 10, 20$ and 50 by the finite deformation theory.

The variations of the mobilized tension in the reinforcement at the center, T_0^* , of the loading, with the intensity of load, q^* , from infinitesimal and finite deformation theories are shown in Fig. 10 for $\beta_s = 10, 20$ and 50 for $G_t^* = 0.1, G_b^* = 0.1, \mu_t = \mu_b = 1.0$ and $\beta_g = 5$. The maximum mobilized tension in the reinforcement increases with increase in β_s , for any particular intensity of load, since lower value of ultimate bearing capacity, leads to larger settlement and mobilization of tension in the reinforcement. The mobilized tensions in the reinforcement for different values of β_s , by the infinitesimal theory are close to each other, since the differences in settlement are relatively very small. The mobilized maximum tension – stress intensity curves from the finite deformation theory are concave upwards

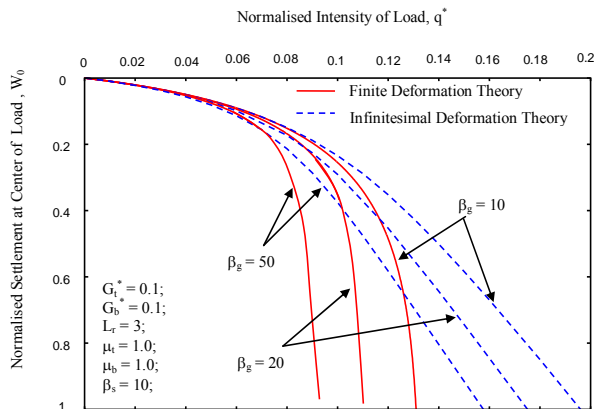


Fig. 11 Intensity of load, q^* – settlement, W_0 , responses: effect of β_g

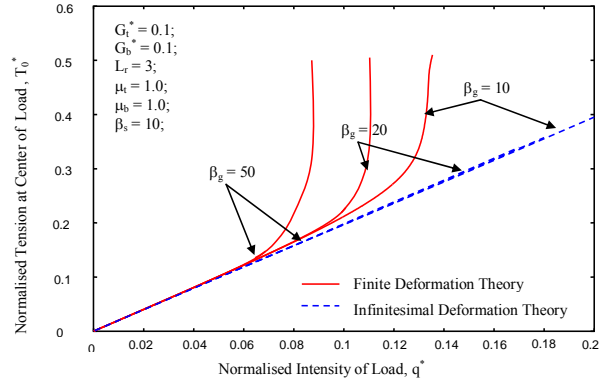


Fig. 12 Intensity of load, q^* - tension, T_0^* responses: effect of β_g

since the granular fill reaches its ultimate load capacity resulting in the reinforcement transferring the load actively to the region outside the loaded width leading to greater increase in maximum mobilized tension.

The influence of the ultimate shear resistance, τ_f , of the granular fill on the intensity of load – settlement responses with uniform loading of the reinforced granular fill – soft ground system, is studied through the parameter β_g , by both finite and infinitesimal deformations theories, for $\beta_g = 5, 10, 20$ (Fig. 11) for $G_t^* = 0.1, G_b^* = 0.1, \mu_t = \mu_b = 1.0$ and $\beta_s = 50$. The differences in the curves based on the two approaches increase with increase in intensity of load. Infinitesimal theory underestimates the settlements as stated before compared to those from the finite deformation theory, especially at large intensities of loads and for large values of β_g . The intensity of load – settlement response curves shift towards the left with increasing β_g , indicating increases in settlements for any particular intensity of load, q^* . The slopes of the load – settlement curves become steeper, indicating that the settlement increases and the ultimate bearing capacity of the footing on the reinforced bed decreases with increasing values of β_g . For uniform load of intensity, $q^* = 0.065$, the maximum settlements at the center of the footing based on finite deformation approach are 0.1033, 0.1086, 0.1295 respectively for β_g equal to 10, 20 and 50.

The intensity of load – maximum mobilized tension responses of the footing for $\beta_g = 5, 10$ and 20 are presented in Fig. 12 for $G_t^* = 0.1, G_b^* = 0.1, \mu_t = \mu_b = 1.0$ and $\beta_s = 50$. For uniform load of intensity, $q^* = 0.065$, the maximum tensions at the center of the loading, T_0^* , are 0.1325, 0.1335, 0.1353 respectively for β_g equal to 10, 20 and 50. The tension increases marginally with increase in β_g . Granular beds with high values of β_g , fail by punching at low bearing stresses resulting in low values of normalized maximum tension. On other hand, stiffer granular beds ($\beta_g \leq 10$) carry larger loads, distribute the same over larger widths and generate

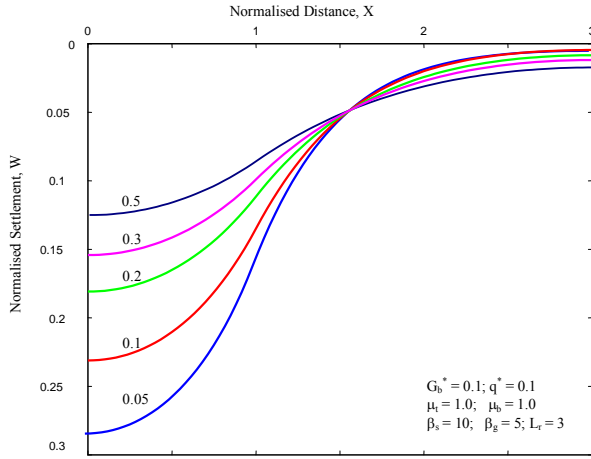


Fig. 13 Settlement profiles: effect of G_t^*

higher tensions in the reinforcement especially closer to the ultimate load carrying capacity values.

Effect of shear stiffness, G_t^* , of the granular fill above the reinforcement on the settlement profile of the granular reinforced bed is studied in Fig. 13. Five values of shear stiffnesses, G_t^* (0.05, 0.1, 0.2, 0.3 and 0.5) are considered with $G_b^* = 0.1$, $\beta_s = 10$, $\beta_g = 5$, $\mu_t = \mu_b = 1.0$ and $q^* = 0.1$. For values of G_t^* increasing from 0.05 to 0.1, 0.2, 0.3 and 0.5, the normalized settlements decrease from 0.282 to 0.231, 0.181, 0.154 and 0.125, and from 0.159 to 0.135, 0.111, 0.099 and 0.085 respectively at the center, $X = 0$, and at the edge of the loading, $X = 1$. The normalized settlements at the edge of the reinforced zone, $X = 3$, increase from 0.0027 to 0.0046, 0.0084, 0.0118 and 0.0175 respectively for G_t^* increasing from 0.05 to 0.1, 0.2, 0.3 and 0.5. The normalized differential settlement between the center and the edge of the loading decreases from 0.123 to 0.04 for G_t^* increasing from 0.05 to 0.5. Differential settlement decreases with the increase in G_t^* , reflecting the ability of the granular fill to distribute the loads more uniformly over a wider area.

For uniform intensity of load, $q^* = 0.1$, the tensions developed in the reinforcement with shear stiffnesses, $G_t^* = 0.05, 0.1, 0.2, 0.3$ and 0.5 of the fill are presented

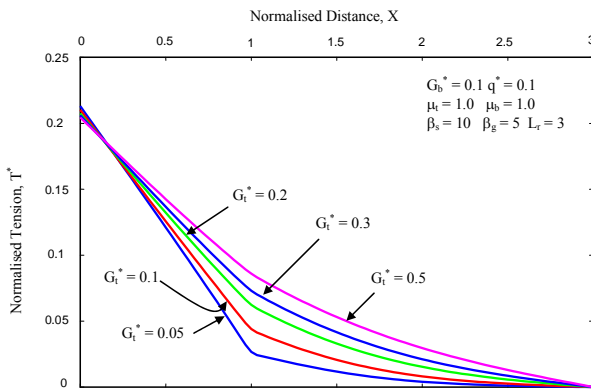


Fig. 14 Tension profiles: effect of G_t^*

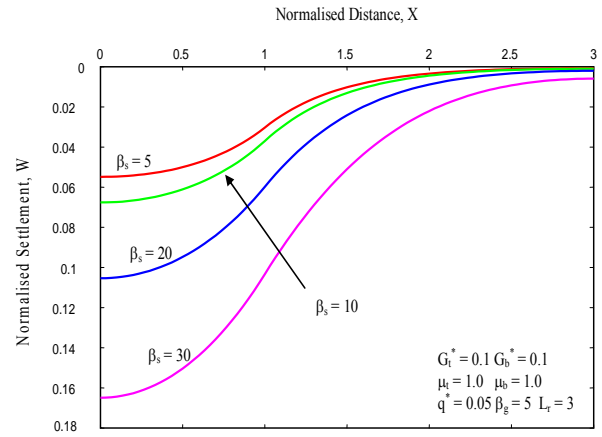


Fig. 15 Settlement profiles: effect of β_s

in Fig. 14 for $G_b^* = 0.1$, $\beta_s = 10$, $\beta_g = 5$ and $\mu_t = \mu_b = 1.0$. The normalized tensions are 0.213, 0.210, 0.207, 0.206 and 0.204 respectively at the center of the reinforcement (i.e., $X = 0$) and 0.0267, 0.0441, 0.0623, 0.073 and 0.086 respectively at the edge of the loading (i.e., $X = 1$) for $G_t^* = 0.05, 0.1, 0.2, 0.3$ and 0.5. The tension in the reinforcement increases beyond the loaded area because with increasing shear stiffness of the fill, the load gets distributed to the area beyond the load leading to an increase in normal and the corresponding frictional stresses along the reinforcement and an increase in the mobilized tension in the reinforcement. The tension at the center of the loaded area and the slopes of the tension profiles decrease marginally with increasing shear stiffness of the granular fill because stiff granular fill distributes the loads more uniformly. Larger stresses are distributed beyond the loaded region causing less differential settlements, leading to smaller mobilized tensions in the reinforcement under the loaded region.

Settlement profiles for $\beta_s = 5, 10, 20$ and 30 for $G_t^* = 0.1$, $G_b^* = 0.1$, $\beta_g = 5$, $\mu_t = \mu_b = 1.0$ and $q^* = 0.05$ are presented in Fig 15. The non-linearity parameter, β_s , of the reclaimed soil has significant effect on the settlement profile of the reinforced granular bed. For $\beta_s = 5, 10, 20$ and 30, the normalized settlements are 0.0549, 0.0676, 0.1054 and 0.1649 respectively at the center of the loading, $X = 0$, 0.0303, 0.037, 0.0598 and 0.1033 respectively at the edge of the loading, $X = 1$, and 0.0007, 0.001, 0.002 and 0.006 respectively at the edge of the reinforced zone, $X = 3$. The settlement increases with increasing β_s , ($= k_s B/q_u$). An increase of β_s implies a decrease of the ultimate bearing capacity, q_{us} , of the reclaimed ground for constant k_s and 'B'. The differential settlement between the center and the edge of the loading increases from 0.0246 to 0.0616 for β_s increasing from 5 to 30.

Figure 16 shows the effect of non-linearity parameter, β_s on the variation of tension in the reinforcement for $\beta_s = 5, 10, 20$ and 30 and for $G_t^* = 0.1$,

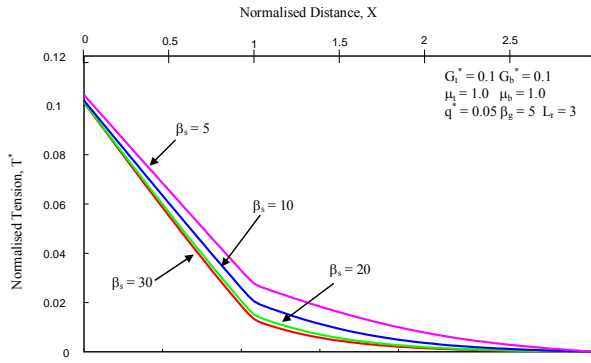


Fig. 16 Tension profiles: effect of β_s

$G_b^* = 0.1$, $\beta_g = 5$, $\mu_t = \mu_b = 1.0$ and $q^* = 0.05$. With increasing β_s from 5 to 30, a six fold increase, the tension at the center of the loading, $X = 0$, increases marginally from 0.1011 to 0.1042, i.e., only by 3%. This small increase is attributed to the increase in differential settlement between the center and the edge of the loading.

The effect of ultimate shearing resistance, τ_f of the granular fill on the settlement profile for a uniform intensity of load, $q^* = 0.05$ is studied (Fig. 17) through the parameter, $\beta_g (= G_p/\tau_f)$ for $\beta_g = 5, 10, 20$ and 30 for $G_t^* = 0.1$, $G_b^* = 0.1$, $\beta_s = 10$, $\mu_t = \mu_b = 1.0$. The normalized settlement increases marginally from 0.0676 to 0.0716 at the center, $X = 1$, while remaining nearly constant at the edge of the loaded region, $X = 1$, for β_g increasing from 5 to 30. This small increase in settlement is accounted for by the decrease in shear resistance of the granular fill. With a decrease in the shear resistance of the granular fill, its ability to transfer load to adjacent layers decreases leading to a smaller amount of load being transferred to outside the loaded region, resulting in a reduction in settlement therein and to an increase of settlement within the loaded region as depicted in Fig. 17.

Figure 18 shows the effect of β_g , the parameter representing the effect of ultimate shear resistance of the granular fill, on the mobilized tension in the

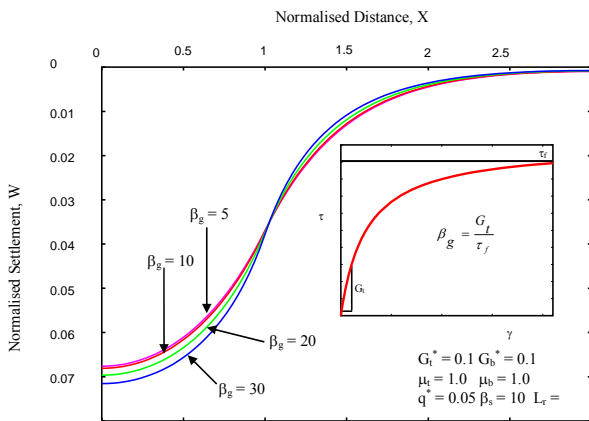


Fig. 17 Settlement profiles: effect of β_g

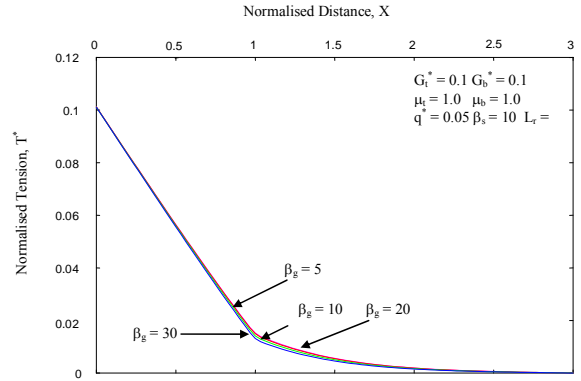


Fig. 18 Tension profiles: effect of β_g

reinforcement ($\beta_g = 5, 10, 20$ and 30) for $G_t^* = 0.1$, $G_b^* = 0.1$, $\beta_s = 10$, $\mu_t = \mu_b = 1.0$ and $q^* = 0.05$. The effect of β_g is very less on the mobilized tension curves, may be because of the small intensities of load considered. The normalized tension at the edge of the loaded region, $X = 1$, decreases from 0.0152 to only 0.01315. As an increase of β_g indicates a decrease in the shear resistance of the granular fill, the load distributed to the outside region reduces causing a reduction in tension in that region as shown in Fig. 18.

CONCLUSIONS

In the present paper, a finite deformation theory is proposed for the analysis and study of the response a reinforced foundation bed on super-soft reclaimed ground incorporating non-linear stress-displacement response of super soft soil and non-linear shear stress – shear strain response of granular fill. The model consists of Pasternak shear layer, rough membrane and elastoplastic Winkler springs to represent the granular fill, the reinforcement layer and the super-soft soil respectively. Formulation is presented for a uniformly loaded strip footing. In this model, full interface friction, μ , ($= \tan \phi$) is assumed to be mobilized at the top and the bottom faces of the reinforcement. Results from both infinitesimal and finite deformation theories are obtained and compared to highlight the importance of the finite deformation theory.

Parametric study carried out highlights the relevance and appropriateness of the finite deformation theory and quantifies the effects of all the relevant parameters on the settlement response of the footing for uniform loading. Settlements obtained by the infinitesimal theory are always considerably less than those from the finite deformation theory. As in the Madhav & Ghosh model, the stress – displacement and stress – tension response curves show negligible differences in the values obtained by both finite deformation and infinitesimal deformation

theories at small intensities of loads. However, the differences increase at larger loads. The most significant finding of the present investigation is the modification in stress – settlement response towards punching type failure suggested by Meyerhof (1974) for soft granular beds.

The settlement of the reinforced granular bed on soft clay and the tension mobilized in the geosynthetic reinforcement are intrinsically related to each other. Stiff granular bed functions as relatively more rigid and facilitates transfer of applied load to the area outside of the loaded region. Larger the normal stresses transferred to the granular fill, the more would be the shear stresses mobilized therein and lead to higher tension in the reinforcement. The reinforced granular bed would settle uniformly reducing differential settlements. The rates of decreases of tension within and outside the loaded regions with respect to G_t^* are inverse of each other. Interestingly, the maximum value of tension mobilized at the centre of the loaded area is nearly independent of G_t^* .

REFERENCES

- Basset, R.H. and Last, N.C. (1978). Reinforcing Earth below Footings and Embankments. Proceedings of the Symposium on Earth Reinforcement, ASCE, 101:1241-1255.
- Binquet, J. and Lee, K.L. (1975). Bearing Capacity Analysis of Reinforced Earth Slabs. Journal of Geotechnical Engineering Division, ASCE, Vol. 101, No GT12: 1257-1276.
- Boutrup, E. and Holtz, R.D. (1983). Analysis of Embankments on Soft Ground Reinforced with Geotextiles. Improvement of Ground, Proceedings of 8th European Conference on SMFE, Ed. by H.G.J. Rathmayer, and K.H.O. Saari, Helsinki, 2: 469-472.
- Ghosh, C. and Madhav, M.R. (1994a). Settlement Response of Reinforced Shallow Earth Bed, Geotextiles and Geomembranes. Vol.13, No.5: 643-656.
- Ghosh, C. and Madhav, M.R. (1994b). Reinforced Granular Fill – Soft Soil System - Membrane Effect. Geotextiles and Geomembranes, Vol.13, No.5: 743-759
- Giroud, J.P. and Noiray, L. (1981). Geotextile Reinforced Unpaved Road Design. Journal of Geotechnical Engineering Division, ASCE, Vol. 107, No. GT9: 1223 – 1254.
- Jarrett, J.M. (1980). Large Scale Tests on Gravel – Fabric – Peat System. Proceedings of Canadian Symposium on Geotextiles, Calgary: 101 – 111.
- Kondner, R.L. (1963). Hyperbolic Stress – Strain Response: Cohesive Soils. Journal of Soil Mechanics and Foundations Division, ASCE, Vol. 89, No. SM1:115 – 143.
- Madhav, M.R. and Poorooshasb, H.B. (1988). A New Model for Geosynthetic Reinforced Soil. Computers and Geotechnics, Vol.6, No.4: 277 – 290.
- Meyerhof, G.G. (1974). Ultimate Bearing Capacity of Footings on Sand Layer Overlying Clay. Canadian Geotechnical Journal, No 2:223 – 229.
- Milligan, G.W.E., Jewell, R.A., Houlsby, G.T. and Burd, H.J. (1989). A New Approach to the design of unpaved Roads. Ground Engineering, 22(3): 25-29.
- Nieuwenhuis, J.D. (1977). Membranes and the Bearing Capacity of Road Bases. Proceedings of the International Conference on the Use of Fabrics in Geotechnics, Paris: 3 – 8.
- Ramu, K. (2001). Modelling Approaches for & Analysis of Reclamation Process and Response of Reclaimed Ground. Ph.D. Dissertation, Indian Institute of Technology, Kanpur, India.
- Shukla, S.K. and Chandra, S. (1994a). The Effect of Prestressing on the Settlement Characteristics of Geosynthetic Reinforced Soil. Geotextiles and Geomembranes, Vol. 13: 531-543.
- Shukla, S.K. and Chandra, S. (1994b). A Generalised Mechanical Model for Geosynthetic Reinforced Foundation Soil. Geotextiles and Geomembranes, Vol. 13: 813-825.
- Terzaghi, K. (1955). Evaluation of Coefficients of Subgrade Reaction. Geotechnique, 5(4):297-326.
- Vidal, H. (1966). La Terre Armee (un nouveau materiau pour les travaux publics). Annales d' ITBTP, July-Aug.: 223-224.
- Yang, Z. (1972). Strength and Deformation Characteristics of Reinforced Sand. Ph. D. Dissertation, University of California at Los Angeles.
- Yin, J.H. (1997a). Modelling Geosynthetic Reinforced Granular Fills Over Soft Soil. Geosynthetic International, Vol. 4, No. 2: 165-185.
- Yin, J.H. (1997b). A Nonlinear Model of Geosynthetic-Reinforced Granular Fill Over Soft Soil. Geosynthetics International, Vol. 4, No. 5: 523-537.
- Yin, J.H. (2000). Comparative Modeling Study of Reinforced Beam on Elastic Foundation. Journal of Geotechnical and Geoenvironmental Engineering, ASCE, Vol. 26, No.3: 265-271.